JOURNAL OF MATERIALS SCIENCE 20 (1985) 2029–2037

Friction and wear properties of monolithic silicon-based ceramics

D. C. CRANMER *
Bendix Advanced Technology Center, Columbia, MD 21045, USA

Friction and wear properties of two forms of silicon nitride (reaction bonded and hot pressed) and two of silicon carbide (reaction sintered and sintered) are reported. The materials were slid against themselves under unlubricated conditions. Tests were run using a simulated inertial sample dynamometer. Sliding speeds ranged from 0.5 to 5.5 m sec^{-1} with applied loads of 225 or 450 N. Friction coefficients were found to be in the range of 0.15 to 0.8 for both types of material. Friction response was qualitatively correlated with changes in surface chemistry at the sliding interface. Wear rates were of the order of 10^{-14} to 10^{-13} m^3 $(N\,m)^{-1}$, in order-of-magnitude agreement with previous pin-on-disc results reported in the literature. Wear surfaces exhibit plastic deformation, ploughing, and oxide film formation and removal.

1. Introduction

Silicon nitride and silicon carbide are being incorporated in a variety of high-temperature applications (e.g. gas turbine engines). Both have excellent thermal and mechanical properties, but will encounter conditions in which sliding or rubbing contact occur. In order to fully exploit the potential of these materials, an understanding of their tribological responses in relation to their surface characteristics and deformation modes must be developed.

Several previous studies [1–5] have examined the friction and wear behaviour of these materials running against themselves using pin-on-disc techniques. Other studies [6–9] have examined their responses when running against a dissimilar material, e.g. iron. Friction coefficients were generally found to be in the range 0.2 to 0.7 over a temperature range from room temperature to 1000° C for both types of material. Wear rates are generally low, but cannot be directly compared in most cases because of differences in wear measurement techniques (thickness change instead of weight loss), and the inherent differences between tests run on different machines (even if all are of the same type). The most direct comparison can be made between a rotating pin-on-disc apparatus [2] and a reciprocating pin-on-disc machine [3] for a variety of silicon-based ceramics. Using the same materials and material combinations, wear rates vary generally by about an order of magnitude with extreme differences of two orders of magnitude. These discrepancies are the result of differences in test-machine dynamics, as well as compositional differences (e.g. MgO rather than Y_2O_3 additives in Si_3N_4) and microstructural differences. They cannot be satisfactorily explained in detail at the present time.

The wear process is generally described in terms of one or more mechanisms [8, 10, 11]: for example adhesive and abrasive processes, plastic deformation, delamination and fatigue. Any one of these mechanisms can predominante, or several of them combine to determine the features of the wear surface and subsurface. Suh [11] has developed the delamination theory of wear to account for a variety of wear processes such as adhesion, fretting and fatigue as part of the motion and interactions of dislocations in the surface and near-surface regions of the material. A number of theories have been developed recently which attempt to account for wear in brittle solids. Evans [12] developed a theory based on link-up of lateral and surface cracks under the

*Present address: The Aerospace Corporation, PO Box 92 957, Los Angeles, CA 90 009, USA.

0022–2461/85 $03.00 + .12

TABLE I Comparison of wear rates of silicon-based ceramics

Material*		Fabrication method†	Reciprocating [16] (10^{14} m^3 N^{-1} m^{-1})	Rotating [15] (10^{14} m^3 N^{-1} m^{-1})
Si_3N_4	AED	RS	26	3.3
	SN220	S	22	0.2
	NC132	HP	16	0.8
	SN201	RS	–	3.0
	SN501	RS	–	4.8
	EC111S	RS	–	7.0
	EC128	RS	–	0.2
	EC131	HP	–	1.5
SiC	NC203	HP	1.6	0.1
	NC435	RS	1.4	0.3
	EC412	RS	1.4	0.1
	EC422	S	3.1	0.01
	Alpha	S	–	1.6
	KT	RS	–	0.2
	SC401	RS	–	0.2
	SC201	S	–	0.1
Sialon		HP	6.1	0.1

*Material producers: NC = Norton, SN and SC = Kyocera, EC = NTK, Alpha and KT = Carborundum, Sialon = AVCO, AED = Nitrasil.
†HP = hot-pressed, RS = reaction-sintered, S = sintered.

area of contact to generate a wear particle. No one theory can as yet account for all the wear processes which have been observed, but the theories are constantly being modified [13].

The mechanisms of friction and wear are the subject of much study and debate. A recent review [14] summarizes the theories of friction. As regards brittle solids such as ceramics, this review suggests that subsurface deformation should be small unless temperatures where plastic deformation can occur are reached, and that the energy expended in the friction process will be small unless plastic deformation can occur. In addition, the review points out the nature of the stress fields surrounding the area of contact, and indicates the probable formation of microcracks at the interface as sliding takes place. As noted above, these cracks are potential sources of wear particles.

The purpose of the present investigation was to measure the friction and wear properties of two silicon-based ceramics. Measurements were made under conditions that were different from previously reported pin-on-disc studies. The results were interpreted in terms of surface chemistry and morphology as well as friction and thermal response.

2. Experimental procedure

Two different silicon nitrides were initially selected for examination: NC 132,* a hot-pressed material, and NC 350,* a reaction-bonded material. Two different silicon carbides were also chosen, in part because of their apparent uniformity of wear rates in prior testing (see Table I). The materials chosen were NC 430,* a reaction-sintered material which is similar to the NC 435 shown in the table, and sintered Alpha,† a conventionally sintered material. Typical compositions for all four materials are detailed in Table II [15–17].

A ring geometry compatible with the testing apparatus was chosen to provide the sliding interface for analysis. A schematic diagram of the apparatus is shown in Fig. 1. The samples follow a circular path about the centre-line shown, maintaining an approximately constant area of contact. The ring dimensions were 4.5 cm outside diameter (OD), 2.5 cm inside diameter (ID) and 0.6 cm thick, except for the sintered Alpha which was 6.1 cm OD, 4.2 cm ID and 0.6 cm thick. All rings were parallel-ground with 600 grit diamond to control the initial surface profiles. The rings were mounted in a simulated inertial sample dynamometer‡ and run against themselves for

*Norton Co., Worcester, Massachusetts, USA.
†Carborundum Co., Niagara Falls, New York, USA.
‡Link Engineering, Detroit, Michigan, USA, Model D1205-E.

TABLE II Typical chemical analysis and properties of materials used

NC 430		α-SiC		NC 132		NC 430	
SiC	88.5 wt%	SiC	98 wt%	Si_3N_4	~ 94 wt%	Si_3N_4	> 98 wt%
Si	10.6	B	0.6	Mg	0.4 to 0.6		
Fe	0.4	C	1.0	Al	0.2 to 0.3	Al	0.2
Al	0.1	Al	0.06 to 0.09	Fe	0.2 to 0.4	Fe	0.4
B	< 50 ppm	Fe	0.2 to 0.3	Ca	0.006 to 0.03	Ca	0.05
				Mn	0.05	–	
				B	< 0.003	–	
				W	1.5 to 2.0	–	
				O	3.0	O	0.5
				Some Si_2ON_2 and Mg silicates are present in small amounts.			
$\rho \sim 3.0\,g\,cm^{-3}$		$\rho \sim 3.15\,g\,cm^{-3}$		$\rho \sim 3.2\,g\,cm^{-3}$		$\rho \sim 2.4\,g\,cm^{-3}$	
Grain size distribution is bimodal: small Si and SiC are less than 10 μm, large Si is ~ 150 μm.		Grain size is ~ 7 μm.		Grain size is about 2 to 2.5 μm.			

times ranging from 5 to 45 min in drag mode (continuous contact and constant force) with applied loads of 225 or 450 N. Relative sliding speeds ranged from 0.5 to 5.5 m sec^{-1}. Applied force, torque, speed, radial-centre midthickness temperature, and radial-centre back face temperature were measured at 1 Hz during contact. Midthickness and back face temperatures were also measured at 0.5 Hz during a 20 min cool-down after the end of each test.

The tested samples were examined in a scanning electron microscope[§] (SEM). Both the bulk and wear surfaces were examined, and elemental chemistry determined by Energy Dispersive X-ray Spectroscopy[¶] (EDXS). The chemical analysis unit was operated in the ultrathin window mode (UTW) to allow determination of oxygen, nitrogen, carbon, and boron contents. The window is a 7.5 μm thick beryllium plate and the unit is operated at a vacuum of $\sim 10^{-9}$ atm (10^{-4} Pa). Intensity corrections were made for the signals using the Kevex-supplied software, and compared with manufacturer's data on unworn specimens. The agreement was excellent (within 0.5 wt%) on all the materials. The same correction was applied to the worn samples. The worn-sample values should not be taken as absolute, since the tortuous nature of the surface may influence the intensity of the X-rays which reach the detector. The corrected results were used to correlate the surface chemistry and morphology with the friction and wear response.

Wear was determined by measuring the change in thickness of the samples. The change in thickness was converted to a normalized wear rate according to [2] and [3] as follows:

$$W^* = V/LD \quad (1)$$

where W^* is the wear rate in $m^3\,(N\,m)^{-1}$, V is the volume lost, L is the applied load, and D is the total distance slid. The volume of material lost is the change in thickness times the area of contact, assuming uniform wear across the entire surface.

3. Results and discussion

3.1. Friction coefficient

Friction coefficients were calculated from the applied force and torque values sampled at 1 sec intervals, and the average and standard deviation of these values calculated. Typical response curves for identical nominal conditions are shown in Figs. 2a–d for the sintered SiC, reaction-sintered SiC, hot-pressed Si_3N_4 and reaction-bonded Si_3N_4, respectively. The important point to note from the figure is that there is no one value of friction coefficient which describes the behaviour of these materials. Any theory which is developed to describe the friction response must take this variability into account. Table III summarizes the friction coefficients obtained for all four materials

[§]ISI, Inc., Santa Clara, California, USA, Model DS 130.
[¶]Kevex Corp., Foster City, California, USA, Model 3500.

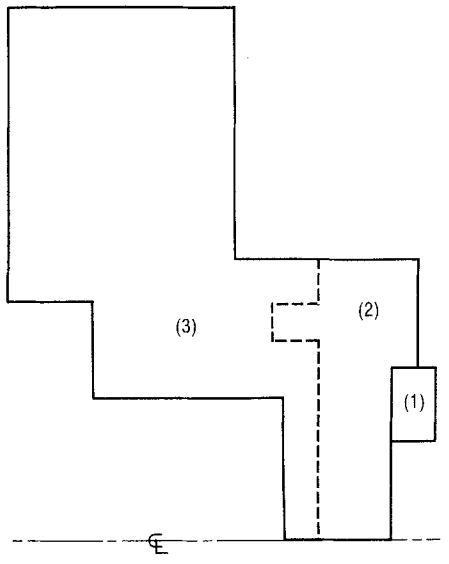

Figure 1 Schematic diagram of wear test rig. 1. Sample; 2. Sample holder; 3. Adapter plate.

TABLE III Friction response of SiC and Si_3N_4

Material	Speed (m sec^{-1})	Friction coefficient
α SiC	0.5	0.44 ± 0.08
	0.9	0.41 ± 0.08
	1.4	0.41 ± 0.05
NC 430	0.5	0.49 ± 0.07
	0.9	0.49 ± 0.07
	1.4	0.43 ± 0.05
	1.8	0.29 ± 0.06
	2.3	0.21 ± 0.09
	2.8	0.20 ± 0.10
NC 132	0.5	0.25 ± 0.09
	0.9	0.40 ± 0.10
	1.4	0.26 ± 0.15
	1.8	0.24 ± 0.14
	2.3	0.21 ± 0.12
	2.8	0.19 ± 0.15
	3.2	0.17 ± 0.23
NC 350	0.5	0.24 ± 0.09
	0.9	0.28 ± 0.06
	1.4	0.29 ± 0.14

at all the speeds used at the 225 N loading. No significant change in response was noted at the higher load. It is evident from Table III that the SiC materials have a more consistent value of friction coefficient (lower standard deviation) than the Si_3N_4 materials over the entire speed range, but in general both materials exhibit lower friction coefficients at higher speeds. This apparent effect of speed on the friction response is an effect of increased temperature at the interface, and will be discussed in a later section. It is not clear at present why the hot-pressed Si_3N_4 exhibits a high friction coefficient at a speed of 0.9 m sec^{-1}.

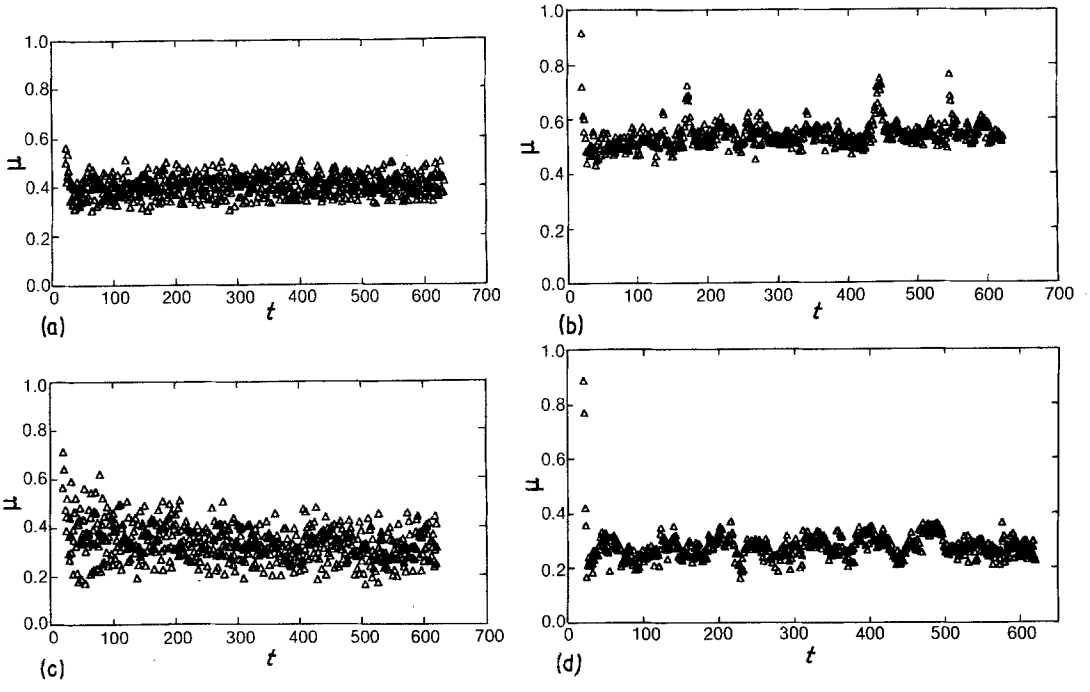

Figure 2 Typical friction responses: (a) sintered SiC, (b) reaction-sintered SiC, (c) hot-pressed Si_3N_4, (d) reaction-bonded Si_3N_4. μ = friction coefficient, t = time.

TABLE IV Experimental wear rates of SiC and Si_3N_4

Material	Wear rate $10^{14}\ m^3\ N^{-1}\ m^{-1}$
α SiC	12.3
NC 430	8.6
NC 132	8.9
NC 350	13.6

The changes in friction response can be correlated with changes in the surface chemistry of the materials as contact occurs. Initially, the reaction-sintered SiC contains < 0.1 wt% oxygen. After sliding contact, the surfaces contain between 0.6 and 10.6 wt% oxygen, with the more severe (higher-speed) conditions generating the higher oxygen content. Based on phase equilibrium considerations, it is expected that the oxygen has been incorporated as SiO_2. A similar phenomenon occurs in hot-pressed Si_3N_4. In this case, the material initially contains about 3 wt% oxygen. After sliding contact, the interface shows oxygen contents ranging from 2.8 to 15.9 wt%, again with the more severe sliding conditions giving the higher oxygen content. In this instance, however, the oxygen may be incorporated in a variety of forms, i.e. SiO_2, complex silicate (due to Mg), or an oxynitride. From the limited data available it is not possible to determine which form is present. However, if it is assumed that both the SiC and Si_3N_4 materials are running on SiO_2 interfacial surfaces, it would be expected that they would have the same friction response. From Table III, this is clearly not the case at lower speeds; thus it must be assumed that they are running on different surfaces, i.e. SiO_2 in the case of SiC and a different phase in the case of Si_3N_4. At higher speeds, the friction coefficients are very similar and it is highly likely that both surfaces are SiO_2.

3.2. Wear behaviour

The calculated wear rates are given in Table IV. Comparison of the results of Table IV with those given in Table I show that the dynamometer results and the pin-on-disc results are within an order of magnitude of one another. Given the differences in the test methods and machine dynamics the agreement must be regarded as good, but it indicates the need for further analytical work in this area.

Figs. 3 (sintered SiC), 4 (reaction-sintered SiC), 5 (hot-pressed Si_3N_4), and 6 (reaction-bonded Si_3N_4) show typical wear surfaces for the four

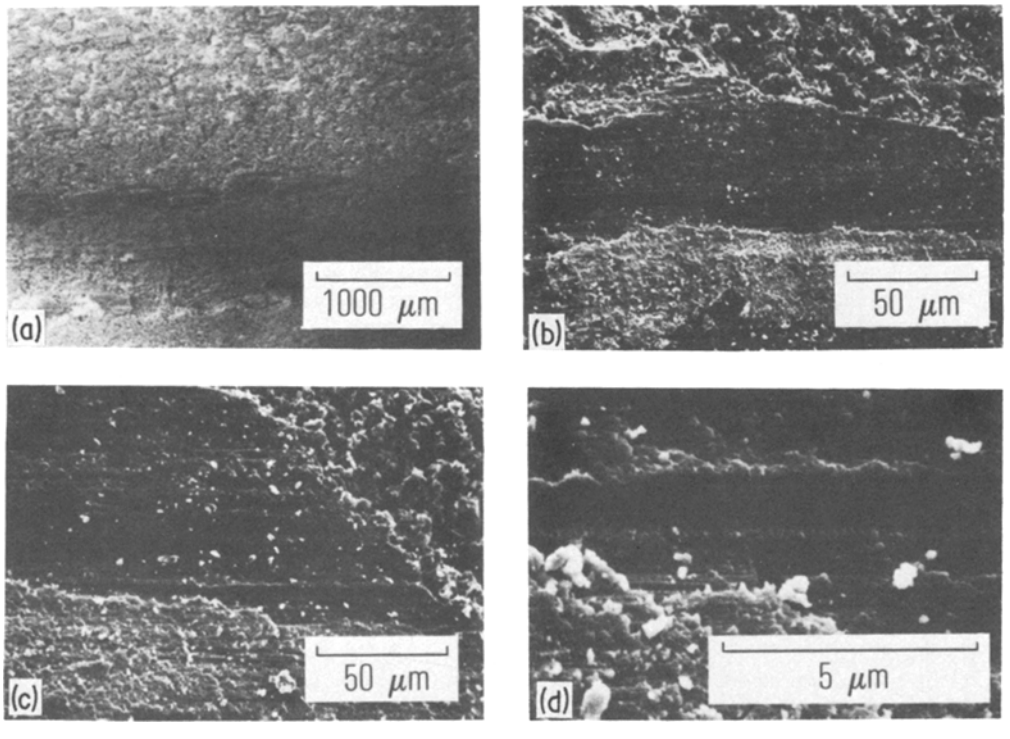

Figure 3 Wear surface of sintered SiC (sintered α): (a) surface plastic deformation, (b) and (c) ploughing and cracking, (d) wear debris, ploughing, and cracking.

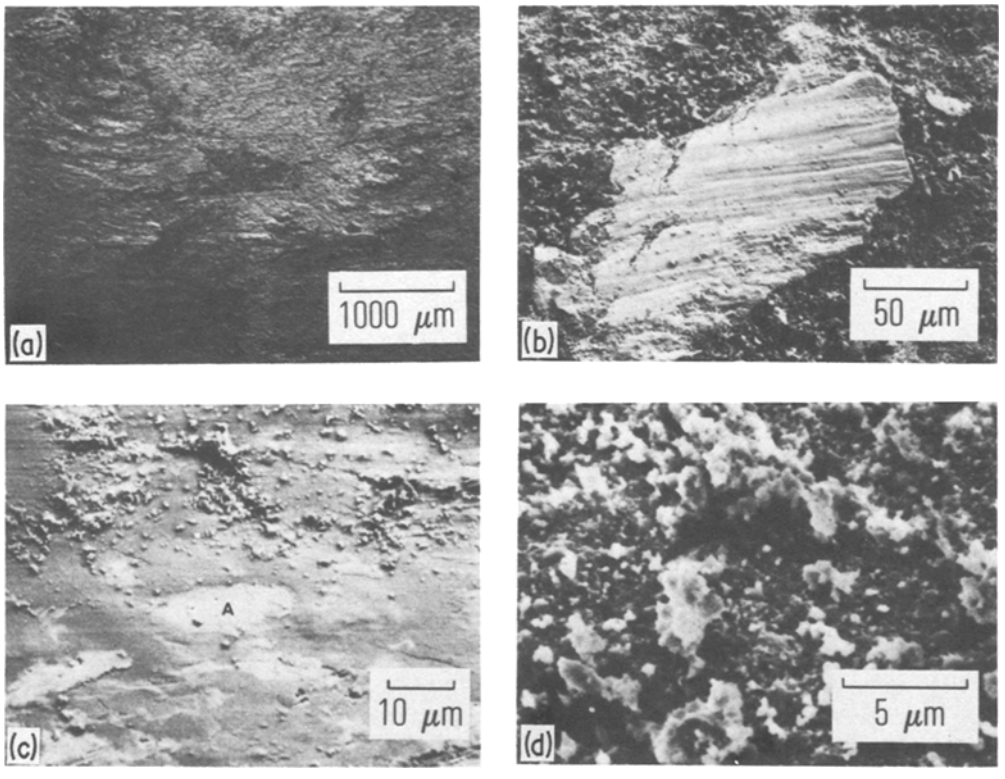

Figure 4 Wear surface of reaction-sintered SiC (NC 430): (a) surface plastic deformation, (b) cracked and ploughed silicon grain, (c) cracking and wear debris (area A is a silicon-rich area), (d) wear debris.

materials tested during the investigation. The conditions of testing are as follows: sintered SiC – 225 N normal load, three ten-minute contact tests at 0.5, 0.9 and 1.4 m sec^{-1}; reaction-sintered SiC – nine tests at 225 N and 0.9 m sec^{-1}, times of contact from 5 to 30 min for a total contact time of 210 min; hot-pressed Si_3N_4 – seven tests at 225 N and 0.9 m sec^{-1}, times of contact from 5 to 20 min for a total contact time of 60 min; reaction-bonded Si_3N_4 – three ten-minute tests at 225 N and speeds of 0.5, 0.9 and 1.4 m sec^{-1}. The conditions for reaction-sintered SiC and hot-pressed Si_3N_4 are similar, while those for sintered SiC and reaction-bonded Si_3N_4 are identical. Sintered SiC (Fig. 3a), reaction-sintered SiC (Fig. 4a) and reaction-bonded Si_3N_4 (Fig. 6a) all show extensive plastic deformation, while hot-pressed Si_3N_4 (Fig. 5a) shows extensive film removal on the same scale. Cracking and ploughing occur in differing degrees in all of the samples as a result of contact. More extensive cracking is evident in the hot-pressed material (Fig. 5b) compared to sintered, reaction-sintered and reaction-bonded materials (Figs. 3b, 4b and 6b). The reaction-sintered SiC contains large silicon grains, one of which is shown in Fig. 4b. These areas exhibit both cracking and ploughing on a larger scale than the surrounding areas. Area A in Fig. 4c is a silicon-rich region as confirmed by EDXS. Each of the materials develops wear debris of the order of 1 to 2 μm or less (Figs. 3d, 4d, 5d, 6d). In all cases the size of the wear debris is less than, or about the same as, the material grain-size. These observations are similar to those seen in a previous study [1] using a conical rider on a flat substrate of the same material.

The types of features shown in Figs. 3 and 4 for silicon carbide occurred in all four of the materials to a greater or lesser extent, depending on the precise conditions of sliding. The film formation and removal shown in the silicon nitride materials (Figs. 5, 6) occurred only in silicon nitride, and only at the more severe sliding conditions. Again, the extent of the film and its removal depend on the sliding conditions.

3.3. Thermal response

A careful examination of Fig. 1 reveals that it is

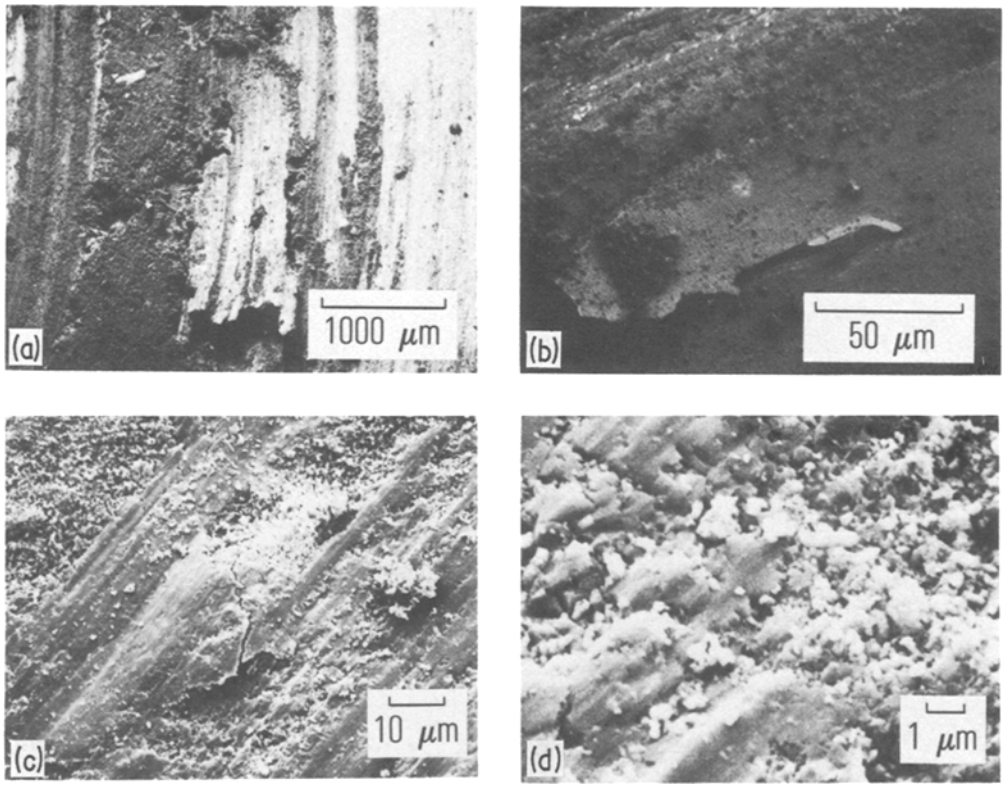

Figure 5 Wear surface of hot-pressed Si_3N_4 (NC 132): (a) cracked surface film, (b) delamination of film, (c) cracking and ploughing of surface, (d) wear debris and plastic deformation.

virtually impossible to directly measure the interface temperature during sliding without affecting that temperature. One method of determining the temperature of the interface is to measure the temperature at several places in the bulk of the sample, and couple these measurements with a finite-difference model to predict an average interface temperature. The two temperatures chosen for measurement occurred at the radial-centre midthickness (in the centre of the Sample 1 in Fig. 1) and the radial-centre midback face (centred on the sample between the Sample 1 and Sample holder 2). Temperature values were generated using the finite-difference model coupled with the thermal properties of the sample, sample holder and adapter plate. Because the sample, sample holder and adaptor plate do not conduct heat perfectly, the model was refined until the model values agreed with the measured values at both locations. The refined model was then used to predict the average interface temperature. Fig. 7 shows both the experimentally determined midthickness temperature and the model predictions (based on constant torque) for the first 400 sec of a hot-pressed Si_3N_4 test (450 N, 0.9 m sec^{-1}, 10 min). The agreement of the experimental and model back face temperatures (not shown for simplicity) is approximately the same as that shown for the midthickness, but occurs about 50 to 75° C lower. From the plot of temperature against time, it can readily be seen that the average interface temperature does not exceed 450° C in this period. The predicted midthickness temperature does not exceed 350° C, and based on the experimental data this represents the maximum midthickness temperature for this test. In principal, the model can be expanded [18] to predict the flash temperatures occurring at the interface.

As noted earlier, there appears to be an effect of speed upon the friction response based on the data in Table III. However, the increase in speed also results in an increase in temperature, as shown in Fig. 8 for a series of tests on the reaction-sintered SiC. Although not shown in the figure, the thermal response for a 1.4 m sec^{-1} velocity falls about midway between those for 0.9 and

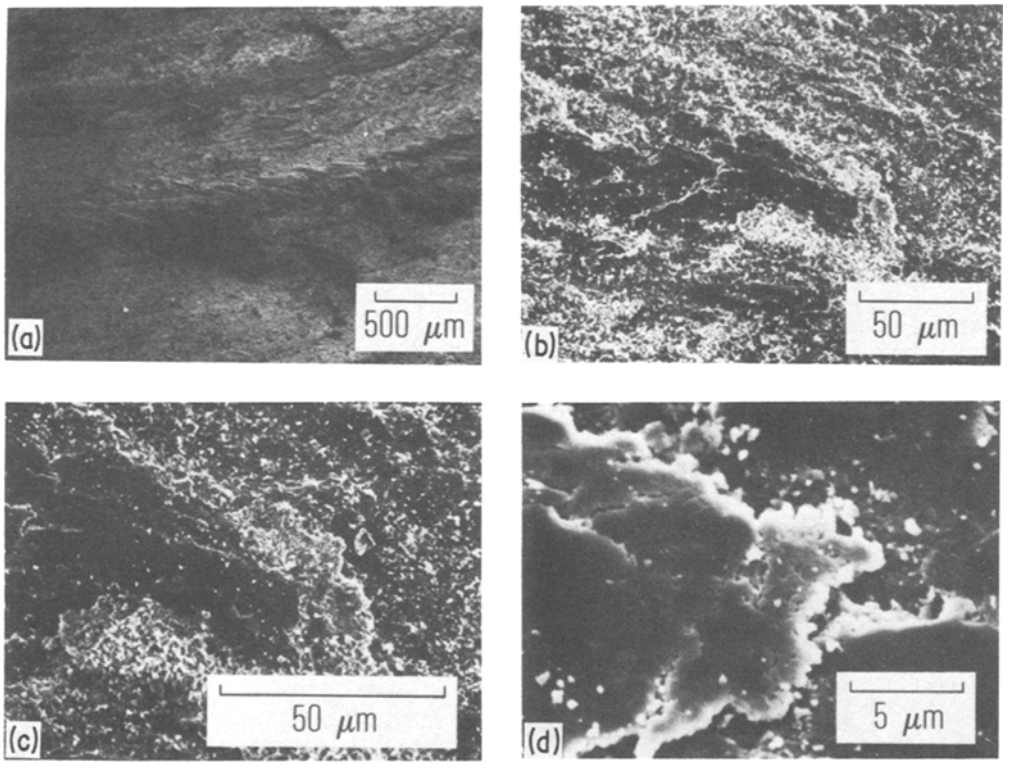

Figure 6 Wear surface of reaction-bonded Si_3N_4 (NC 350): (a) surface plastic deformation, (b) and (c) cracking and surface film, (d) film removal and wear debris.

1.8 m sec^{-1}. The increase in temperature is due to the increased energy which is dissipated as the speed increases, and results in easier plastic deformation or viscous flow of the phases present at the interface; this leads to the observed decrease in the friction coefficient. The temperature rise will be a complex function of the thermal properties of the materials, the kinetics of film formation, and the surface topology. There is no model available at present to describe this behaviour in terms of these parameters.

4. Conclusions

Friction coefficients of the silicon-based ceramics tested range from 0.15 to 0.8. Wear rates vary from 10^{-14} to 10^{-13} $m^3(N\,m)^{-1}$, in order-of-magnitude agreement with previous results. Friction response can be qualitatively correlated with

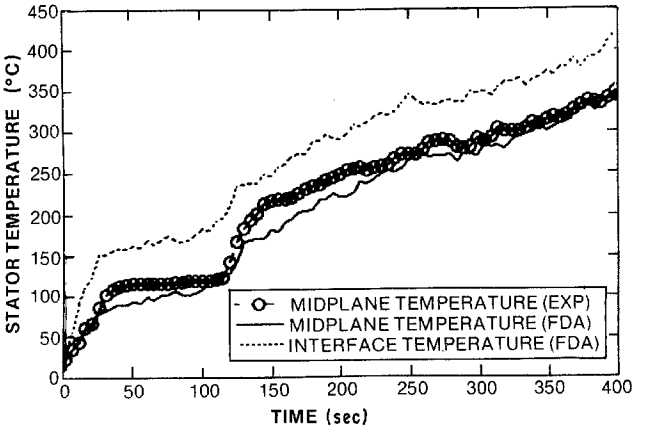

Figure 7 Comparison of temperatures predicted by finite-difference analysis (FDA) of heat flow, and experimentally measured temperatures (EXP) in Si_3N_4 (NC 132).

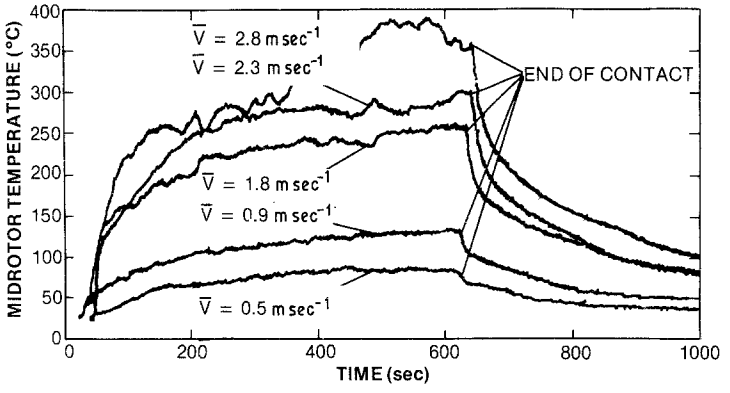

Figure 8 Change in midthickness temperature with speed in reaction-sintered SiC (NC 430).

surface chemistry. Evidence of plastic deformation, cracking and ploughing have been seen in all the materials investigated.

Acknowledgements

The author would like to thank Dr J. Ku for performing the finite-difference analysis of thermal response, and Drs J. Roberts and H. Price for their discussions and critical reading of the manuscript. He would also like to thank D. Urech for performing the required microscopy.

References

1. O. O. ADEWOYE and T. F. PAGE, *Wear* **70** (1981) 37.
2. F. J. CARIGNAN and A. I. WEST, "Hard-on-Hard (Ceramic) Long-Life Seals and Riders for Cryogenic Coolers", Final Report, US Air Force Report AFWAL-TR-81-4060, August 1981.
3. A. I. WEST and F. CARIGNAN, "Evaluation of Improved Materials for Stationary Diesel Engines Operating on Residual and Coal Based Fuels", Final Report, US DOE Contract AC03-79ET15 444, July 1980.
4. J. C. SIKRA, J. E. KRYSIAK, P. R. EKLUND and R. RUH, *Amer. Ceram. Soc. Bull.* **53** (1974) 581.
5. E. F. FINKIN, S. J. CALABRESE and M. B. PETERSON, *Lubr. Eng.* (May 1973) 197.
6. K. MIYOSHI, D. BUCKLEY and M. SRINIVASAN, "Tribological Properties of Sintered Polycrystalline and Single Crystal Silicon Carbide", NASA Technical Memo. 82 829, May 1982.
7. K. MIYOSHI and D. H. BUCKLEY, "Surface Chemistry and Wear Behavior of Single-Crystal Silicon Carbide Sliding Against Iron at Temperatures to 1500° C in Vacuum", NASA Technical Paper 1947, February 1982.
8. R. L. MEHAN and S. C. HAYDEN, *Wear* **74** (1981–2) 195.
9. K. MIYOSHI and D. H. BUCKLEY, "Anisotropic Tribological Properties of Silicon Carbide", NASA Technical Memo. 81 547, April 1981.
10. E. RABINOEWICZ, "Friction and Wear of Materials" (Wiley, London, 1966) pp. 125–198.
11. N. P. SUH, *Wear* **25** (1973) 111.
12. A. G. EVANS, "Abrasive Wear in Ceramics: An Assessment", in "The Science of Ceramic Machining and Surface Finishing II", edited by B. J. Hockey and R. W. Rice, NBS Special Publ. 562, 1979.
13. S. CHAING and A. G. EVANS, *J. Amer. Ceram. Soc.* **66** (1983) 4.
14. D. TABOR, *J. Lubr. Tech.* **103** (1981) 169.
15. D. C. LARSEN, "Property Screening and Evaluation of Ceramic Turbine Engine Materials", AFML-TR-79-4188, October 1979.
16. Norton Co., product literature.
17. Carborundum Co., product literature.
18. J. T. KU, private communication, 1983.

Received 26 March
and accepted 26 July 1984